

A remote flow cell for UV absorbance detection with capillary HPLC based on a single strand fiber optic

Houle Wang,[†] Eugene C. Yi, Catherine A. Ibarra and Murray Hackett*

Department of Medicinal Chemistry, University of Washington, Box 357610, Seattle, WA 98195, USA. E-mail: mhackett@u.washington.edu

Received 18th February 2000, Accepted 24th March 2000

Published on the Web 9th May 2000

A remote flow cell based on a single strand of fused-silica fiber optic was built for UV absorbance detection with a packed capillary HPLC system, using commercially available pumps, detection electronics (Shimadzu) and fittings. This 'off-column' flow cell design is applicable to both pressure and electro-osmotically driven systems. The goals were to minimize the linearity and light leakage problems that often limit the performance of UV absorbance detection with capillary chromatography. A linear dynamic range of 10^3 (reserpine, $\lambda = 220$ nm), and a concentration detection limit of 5.1×10^{-8} mol l⁻¹ were observed. Baseline noise was measured at 3.5×10^{-5} absorbance units (AU), with a standard deviation of 1.7×10^{-5} AU. The illuminated volume of approximately 3 nl was optimized for capillaries with inner diameters in the range 50–100 μ m, and flow rates from 100 nl min⁻¹ to 1 μ l min⁻¹. These modifications of readily available instrumentation have allowed the construction of a practical system for fractionating complex mixtures of peptides in small amounts, prior to mass spectrometry or additional wet chemistry steps.

Introduction

A number of approaches to UV spectroscopic detection have been developed for capillary high-performance liquid chromatography (HPLC).^{1–4} A feature they share in common is the use of fused-silica capillary tubing as the body of the flow cell. The tubing can be either that of the separation column itself or a separate piece configured into a 'U cell,' 'Z cell,' etc. The walls of fused-silica tubing, with portions of the outside layer of polyimide cladding removed, also serve as light windows. These designs offer the advantages of being inexpensive and relatively easy to implement. However, they suffer from the difficulties inherent in collimating the UV light such that only the desired portion of the tubing is illuminated.^{3,4} Because the fused-silica tubing functions as both cell body and light window, light leaks from the cell body are hard to avoid. More importantly, if a significant portion of the light passes through the fused-silica, but not the fluid stream containing the analyte, the Beer–Lambert law will no longer hold true and the result will be a non-linear response from the detector. Compared with flow cells built on a larger scale, the relative thickness of the capillary wall is wide compared with the optical path length, especially with the 'on-column' designs, which can be a significant source of light losses. Extreme sensitivity to refractive index perturbations is also common to such small scale optical detection technologies, regardless of which approach is employed. We report here a design conceived with the intention of minimizing the number of optical elements that serve as sources of transmission losses and scattering, in a system intended for practical use in a protein chemistry laboratory.

In order to widen the range of linear detector response, the body of the flow cell should be opaque to UV and visible light. The light beam must be collimated and aligned such that the percentage of photons launched through the entrance optics that actually interact with the analyte stream is maximized. To make such a device that has only a few nanoliters of volume is very

difficult, using the designs common to larger, more easily fabricated analytical or microbore scale flow cells. Larger scale systems typically employ metal flow cell bodies with quartz or sapphire windows, and separate lenses to focus the light in and (or) out of the illuminated portion of the cell. In this work, we utilized a commercial four-port cross fitting for the flow cell body. A pair of fused-silica optical fibers served as entrance and exit light windows. They were in physical contact with the analyte stream itself, rather than the fused-silica walls of the analytical column. Fiber optics in various configurations have been applied to capillary flow cell designs by a number of laboratories. Published work includes an on-column detector for high temperature open tubular column chromatography⁵ and fiber optics used with LED (light emitting diode) light sources.⁶ Renn and Synovec have shown that the use of single fiber optic designs can help minimize the effects of refractive index perturbations.⁷ A similar, but more complex, design was used in our previous work, utilizing fiber optic bundles for UV detection with capillary gas chromatography⁸ and gas-phase UV detection in tandem with mass spectrometry.⁹ The flow cell design reported here is general in its applicability to capillary fluid systems, including HPLC, electrophoresis (CE), electrochromatography (CEC) or flow injection analysis (FIA).

Experimental

Reagents and standards

HPLC grade methanol, acetonitrile (Burdick and Jackson, Muskegon, MI, USA) and trifluoroacetic acid (J. T. Baker, Phillipsburg, NJ, USA) were used as received. The water was from a Barnstead Nanopure UV system (Thermolyne, Dubuque, IA, USA). The peptide and protein sample solutions were prepared in 10% acetic acid in water (by volume) with human angiotensin I and bovine serum albumin (BSA) (Sigma, St. Louis, MO, USA). BSA was digested with sequencing grade modified trypsin (Promega, Madison, WI, USA). Reserpine (Sigma) solutions were made by serial dilution with water–methanol (1 + 1).

[†] Present address: Bruker Daltonics, 15 Fortune Drive, Manning Park, Billerica, MA 01821, USA.

Remote flow cell

The UV flow cell was built into a 1/16 in (1.6 mm) stainless-steel 'cross' fitting (Valco, Houston, TX, USA, part No. MX1XCS6) with a 0.15 mm bore polyetheretherketone (PEEK) insert and stainless-steel ring (Valco), see Fig. 1. The original stainless fittings were retained for the entrance and exit fiber optics, but undyed PEEK fittings (Valco) were used for the liquid inlet and outlet lines. In both cases, sleeves cut from Teflon HPLC tubing (Valco) were used to seal the fused-silica pieces into the fittings. The use of a stainless fitting for the cross was an arbitrary decision. Fittings of the same dimensions are readily available in non-conducting PEEK for workers who may wish to build a similar flow cell for use with CE or CEC, or for use with an electrospray LC-MS system.

A pair of polarization resistant optical fibers, 200 μm core, 220 μm clad and 240 μm buffer (Polymicro Technologies, Phoenix, AZ, USA), were used for transferring UV light to and from the remote flow cell. Less expensive telecommunications grades of fused-silica fiber optic, *i.e.*, optimized for use in the IR, will not tolerate repeated exposure to UV light. The optical fibers were pre-cut and polished by the vendor, in order to make collimation and light throughput as efficient as possible. One bore of the cross was drilled to a 350 μm diameter in order to accommodate a packed capillary column (75 μm id \times 350 μm od) that was inserted into this bore and stopped at the position shown in Fig. 1. A fused-silica capillary, 20 cm long, 10 μm id, 150 μm od (Polymicro Technologies), was used as an exit line (Fig. 1), narrow enough to maintain sufficient back-pressure to avoid outgassing and bubble formation.

UV detector

A Shimadzu SPD-10A UV spectrophotometric detector (Shimadzu, Kyoto, Japan) was modified for use with capillary columns and the remote flow cell. One quartz lens from the

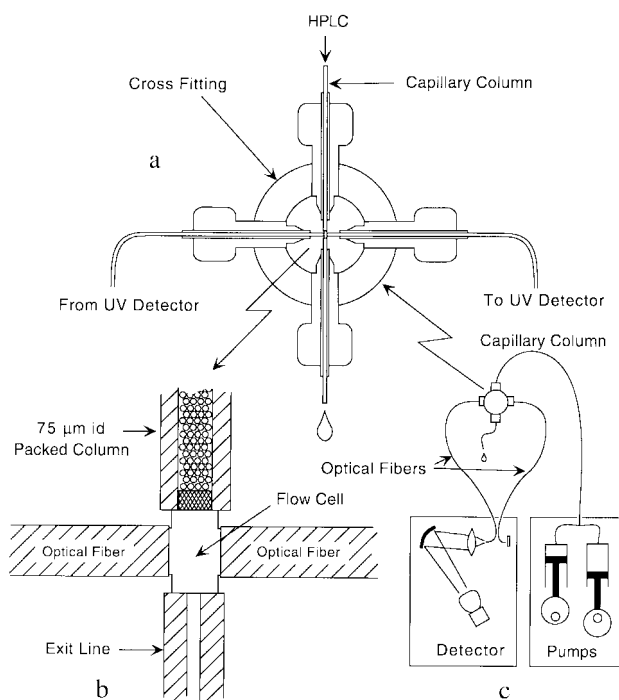


Fig. 1 Diagrams of the single fiber optic remote flow cell design. (a) Arrangement of the fused-silica HPLC column, fluid outlet line and fiber optics in the stainless-steel cross fitting. (b) Close-up of the illuminated portion of the flow cell. (c) Arrangement of the capillaries with respect to the HPLC pumps and UV detector optical bench. For the sake of clarity, the pre-column splitter and other plumbing elements between the pumps and flow cell inlet are not shown.

original semi-micro flow cell assembly (Shimadzu part No. 228-23401-91) was removed and replaced by a GC ferrule (Fig. 2). The optical fiber serving to direct light into the remote flow cell was inserted and aligned to the focus point of the first quartz collimating lens. The photodetector assembly was moved out of the factory standard optical bench to a light-tight chamber fabricated in-house, that allowed more space for positioning the fiber optic (Fig. 2). A PEEK sleeve (Upchurch, Oak Harbor, WA, USA) was used to keep out stray light where the fiber optic enters the photodetector housing (Fig. 2). The SPD-10A uses a standard deuterium bulb as a UV light source. The factory standard 10 k Ω resistor (RM9) was bypassed by a 1 k Ω high precision, low temperature coefficient resistor (Dale, Columbus, NE, USA) to increase the preamplifier gain (channel 1). The reference cell optics and electronics were not modified. The detector was set to 0.05 arbitrary units (AU) full-scale for the capillary chromatography experiments and 2.0 AU for the reserpine calibration. The strip-chart recorder (Model BD40; Kipp and Zonen, Delft, The Netherlands) was used with a 10 mV full-scale deflection input.

Microcapillary HPLC system

Two LC-10AD pump modules (Shimadzu), a low volume mixer (Michrom BioResources, Auburn, CA, USA, part No. 602/25013/03) and a pre-column splitter assembly fabricated in-house, were used for the constant flow binary gradient HPLC system. The split ratio was about 1000:1, as measured at the beginning of the gradient. We used a 40 cm fused-silica packed capillary column (75 μm id \times 350 μm od) packed with 12 cm of either Magic 200 \AA 5 μm C₁₈ (Michrom BioResources) or 8 μm PLRP-S 4000 (Polymer Laboratories, Amherst, MA, USA). Samples were loaded pneumatically using a stainless-steel high-pressure vessel charged with helium at between 500 and 1000 psi (3.52×10^5 – 7.03×10^5 kg m⁻²). The separations were carried out with linear gradients (0–100% acetonitrile over 40–60 min, depending on the specific experiment). The water and acetonitrile contained 0.1 and 0.085% trifluoroacetic acid (TFA) by volume, respectively. Flow rates were typically 200–500 nl min⁻¹, as determined by measuring flows at the outlet capillary with the aid of a disposable micropipet. The linearity of the gradients generated with this type of pre-column splitter arrangement cannot be assumed. They were checked

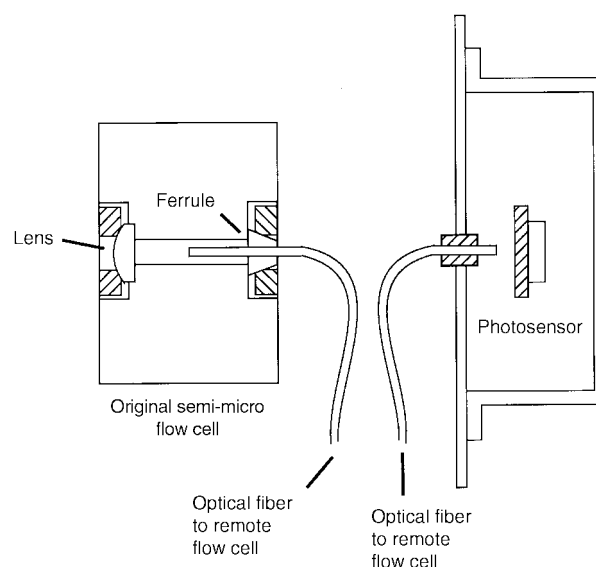


Fig. 2 Structural modifications made to the Shimadzu SPD-10AV detector assembly. Arrangement of (left) the entrance optical fiber mounted in the original semi-micro flow cell (not drawn to scale), and (right) the exit fiber optic and photodetector element in a light-tight housing.

using a linear ramp of increasing acetone concentration. These conditions are appropriate when optimizing the chromatography is not a major concern. When it is a concern, a longer packed length of about 20 cm and a shallower gradient would normally be employed for a more efficient separation. The pre-column splitter and sample loading scheme were based on previously published work^{10,11} as adopted for use with mass spectrometric detection^{12,13} and the off-line fractionation of peptides.¹⁴ Details of the splitter plumbing on the system reported here are virtually identical with those reported previously for the capillary HPLC inlet system to our triple quadrupole mass spectrometer.¹⁵

Results and discussion

Detector noise and drift

A constant flow of 50% acetonitrile in water and 0.085% TFA was pumped through the analytical column at 400 nl min⁻¹. Fig. 3 shows the baseline noise using the remote flow cell to be about 0.035 mAU peak-to-peak at $\lambda = 220$ nm. Drift under these same isocratic conditions was about 1.8 mAU h⁻¹, and was dependent in part on fluctuations in the laboratory ambient temperature and light levels. This level of drift represents about 5% of full-scale with the detector and recorder settings we normally use for peptide analysis. It is likely that these values could be improved slightly by modifying the reference cell optics to give a light path that is closer to that of the remote sample cell. An example would be the use of a fiber optic beam splitter, as we have employed in our previous work with capillary GC.^{8,9} The performance of the present design is adequate for our practical needs. Therefore, we chose to avoid the added complexity of the beam splitter or other modifications to the reference cell. Covering the fiber optics in a light-tight housing leads to lower drift values than those reported above. However, this makes the device less easy to use for practical work. Therefore, we opted to leave them exposed to ambient light for the sake of convenience.

Linear dynamic range, detection limits and precision

Reserpine (M_r 608.69) was measured at ten different concentrations, from 2 $\mu\text{g ml}^{-1}$ to 1.5 mg ml⁻¹ (3.3×10^{-6} – 2.5×10^{-3} mol l⁻¹). For each concentration, three injections were made directly into the flow cell, bypassing the packed column. Between each injection, blank solvent (1 + 1 methanol–water) was used to flush the flow cell. The average of three

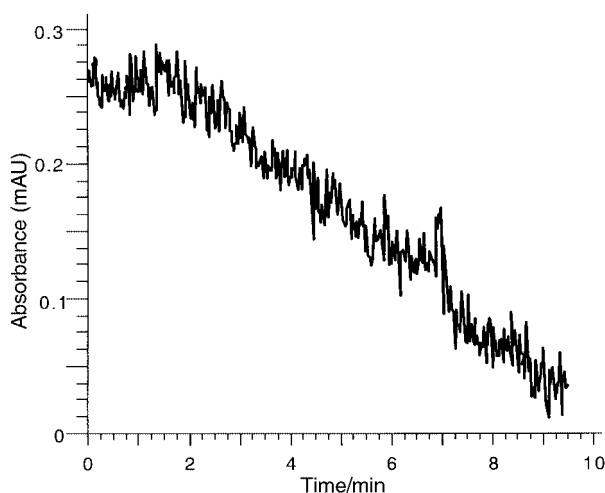


Fig. 3 Noise and drift measured at 220 nm under isocratic conditions, see text for details.

measurements for each concentration is plotted in Fig. 4. The precision (relative standard deviation, RSD) of all points was less than 1%, except at 2 and 5 $\mu\text{g ml}^{-1}$, which were 10 and 4%, respectively. Concentrations of reserpine lower than 2 $\mu\text{g ml}^{-1}$ were not included in the linear dynamic range calculations because we felt them to be of questionable relevance to the analysis of peptides and proteins. Three orders of linear dynamic range were achieved. The practical working range for peptide analysis ($\lambda = 214$ nm) was slightly less, due to the weaker molar absorptivity of the peptide bond, see discussion below. The concentration detection limit calculated from the least-squares fit of the calibration data (Fig. 4) was 0.031 $\mu\text{g ml}^{-1}$ or 5.1×10^{-8} mol l⁻¹. This concentration corresponds to about 160 amol present in a 3 nl volume. These values represent the concentration predicted from the calibration equation (Fig. 4) for an absorbance equal to the y-intercept plus three times the standard deviation of 2 min of baseline noise ($s = 0.017$ mAU). The noise observed with the wash solution between reserpine measurements was essentially identical with that shown in Fig. 3. Reserpine is known to be a strong UV absorber ($\lambda_{\text{max}} = 216$ nm, $\epsilon = 61\,700$, CHCl₃)¹⁶ and represents an unrealistically favorable case from a protein chemist's point of view. Concentration detection limits ($\lambda = 214$ nm) for various peptide and protein standards, e.g., angiotensin I, have fallen in the range from 5×10^{-6} to 5×10^{-5} mol l⁻¹, due to the lower molar absorptivity of the peptide bond ($\lambda_{\text{max}} = 210$ nm, $\epsilon \sim 20$ – 24 , water).^{17,18} The amide bond is a weak chromophore, a fact that is seldom mentioned explicitly in recent literature dealing with HPLC and UV absorbance detection of peptides. UV detection limits are well known to correlate linearly with molar absorptivity, when operating under conditions where the Beer–Lambert law is applicable. Based on this line of reasoning and the statistical treatment of the reserpine data, one would predict detection limits, monitoring at 214 nm, for peptides of the order of 10–100 fmol on-column, similar to what we have observed experimentally under average conditions. This prediction also takes into account the pre-concentration effect that occurs when the analyte is adsorbed onto a stationary phase and eluted as a peak rather than infused at a constant concentration. This tends to be balanced in practice by significant wall losses when working at concentrations of less than 1 pmol μl^{-1} . While not useful for detector characterization *per se*, because one cannot really know the true concentration of analyte in the flow cell when eluting from a column, the experimental on-column data are useful as a guide to what we can expect in our applications work.

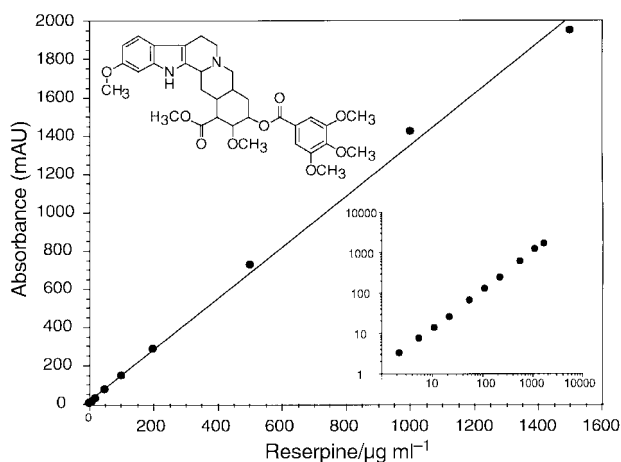


Fig. 4 UV absorbance calibration graph for ten concentrations of reserpine in water ($\lambda = 220$ nm). The inset shows the same data and units plotted on axes incremented as powers of 10. The chemical structure of reserpine is also shown. The unweighted linear least-squares calibration line shown is $A = 1.33 [\text{reserpine}] + 1.53$, $R^2 = 0.997$. Uncertainties in these measurements are discussed in the text.

Direct comparisons with other flow cells, using the same HPLC and detector electronics to control for variations in instrument performance unrelated to the flow cell configuration, have not been made. However, based on the senior author's previous experience with on-column detection and U cells,¹⁴ where RSD values for replicate peak height or peak area measurements were seldom observed to be better than 10%, the calibration data and the tryptic peptide data discussed in the next section are suggestive that there may be better precision with this type of device. We attribute this observation to an optical design with fewer elements and interfaces, which are well known to serve as sources of transmission losses, light scattering^{19,20} and reproducibility problems, especially when working on a nanoliter scale. Less is better. Although there may be a trade-off in terms of signal-to-noise, the relatively short path length that exists ($\sim 150\ \mu\text{m}$) between the polished, parallel faces of the entrance and exit fiber optics may also contribute towards improved precision. A shorter path length provides fewer opportunities for scattering and local variations in temperature, and therefore refractive index, within the cell.

Analysis of peptides and proteins

The separation of $1\ \mu\text{l}$ BSA (M_r 66 424) tryptic digest shown in Fig. 5 was performed with $\sim 1.4\ \text{pmol}$ of digest injected on-column, using 12 cm of the Magic C_{18} material, with a 60 min linear gradient at a flow rate of $400\ \text{nl min}^{-1}$. Most importantly, the BSA data provided verification of flow cell operation under changing refractive index conditions during gradient elution (Fig. 5). The repeatability of the observed signals seems to be related more to errors in the volume injected rather than the flow cell optical properties, and generally falls in the range 3–7% (RSD), for $1\ \mu\text{l}$ injections of tryptic peptide mixtures. We expected little in the way of extra-column band broadening due to the flow cell, given a total cell volume of the order of 4 nl and peak volumes that usually fall in the range 50–100 nl. Observed peak widths are the same when a virtually identical capillary HPLC system, without in-line UV detection, is used as the inlet to our triple quadrupole mass spectrometer. Based on the idea that the total flow cell volume should not exceed one tenth of the peak volume being measured, the cell is probably suitable for

detecting peaks of 40 nl or greater volume, without band broadening attributable to the cell itself.

The system has been used with real samples, including a variety of proteins important in the field of microbial pathogenesis. We use the system for the fractionation of low picomole amounts of proteolytic digests, most commonly prior to either further digestion steps or characterization of molecular weights by matrix-assisted laser desorption/ionization time-of-flight (MALDI-TOF) mass spectrometry.

Acknowledgments

We thank Kerry Nugent and co-workers at Michrom for their insightful comments and generous support, and Darryl J. Bornhop at Texas Tech University for his comments regarding flow cell optics. We thank Weibin Chen for his critical reading of the manuscript. Jeanine M. Kanov assisted with the production of the manuscript. This work was funded under start-up funds from the School of Pharmacy and grant 65-2896 from the Royalty Research Fund of the University of Washington.

References

- 1 Y. Walbroehl and J. W. Jorgenson, *J. Chromatogr.*, 1984, **315**, 135.
- 2 J. P. Chervet, M. Ursem, J. P. Salzmänn and R. W. Vannoot, *J. High Resolut. Chromatogr.*, 1989, **12**, 278.
- 3 J. P. Chervet, R. E. J. Vansoest and M. Ursem, *J. Chromatogr.*, 1991, **543**, 439.
- 4 M. T. Davis and T. D. Lee, *Protein Sci.*, 1992, **1**, 935.
- 5 L. M. Svensson and K. E. Markides, *J. Microcol. Sep.*, 1994, **6**, 409.
- 6 C. T. Culbertson and J. W. Jorgenson, *Anal. Chem.*, 1998, **70**, 2629.
- 7 C. N. Renn and R. E. Synovec, *Anal. Chem.*, 1991, **63**, 568.
- 8 D. J. Bornhop, L. Hlousek, M. Hackett, H. Wang and G. C. Miller, *Rev. Sci. Instrum.*, 1992, **63**, 191.
- 9 M. Hackett, H. Wang, G. C. Miller and D. J. Bornhop, *J. Chromatogr. A*, 1995, **695**, 243.
- 10 R. T. Kennedy and J. W. Jorgenson, *Anal. Chem.*, 1989, **61**, 1128.
- 11 M. A. Moseley, L. J. Deterding, K. B. Tomer and J. W. Jorgenson, *Anal. Chem.*, 1991, **63**, 1467.
- 12 D. F. Hunt, J. E. Alexander, A. L. McCormack, P. A. Martino, H. Michel, J. Shabanowitz, N. Sherman, M. A. Moseley, J. W. Jorgenson, L. J. Deterding and K. B. Tomer, in *Techniques in Protein Chemistry II*, ed. J. J. Villafranca, Academic Press, New York, 1991, p. 441.
- 13 K. B. Tomer, M. A. Moseley, L. J. Deterding and C. E. Parker, *Mass Spectrom. Rev.*, 1994, **13**, 431.
- 14 M. Hackett, R. C. Hendrickson, R. Falchetto, C. B. Walker, J. Shabanowitz and D. F. Hunt, in *Proceedings of the 46th ASMS Conference on Mass Spectrometry and Applied Topics*, American Society for Mass Spectrometry, Atlanta, GA, 1995, p. 441.
- 15 H. Wang, K. B. Lim, R. F. Lawrence, W. N. Howald, J. A. Taylor, L. H. Ericsson, K. A. Walsh and M. Hackett, *Anal. Biochem.*, 1997, **250**, 162.
- 16 Product information provided by Sigma Chemical Co., St. Louis, MO.
- 17 D. M. Kirschenbaum, *Anal. Biochem.*, 1975, **68**, 465.
- 18 R. K. Scopes, *Anal. Biochem.*, 1974, **59**, 277.
- 19 M. Born and E. Wolf, *Principles of Optics*, Cambridge University Press, Cambridge, 7th edn., 1999.
- 20 W. J. Smith, *Modern Optical Engineering*, McGraw-Hill, Boston, MA, 2nd edn., 1990.

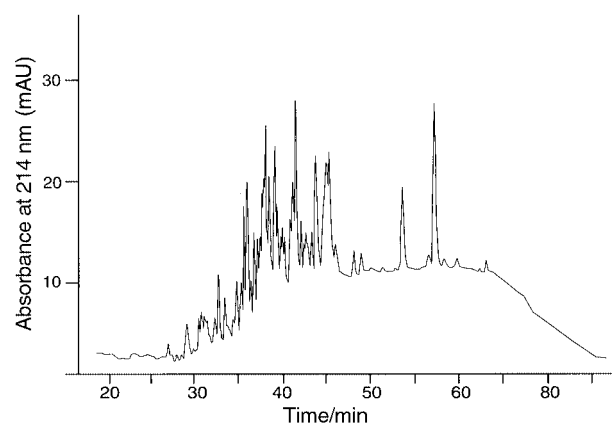


Fig. 5 Capillary HPLC separation of a tryptic digest of BSA. Conditions are given in the text.